The Occurrence of Rupture in Deep-Drawing of Paperboard

Malte Wallmeier,* Marek Hauptmann, and Jens-Peter Majschak

The production of paperboard packaging components in fast-running machines requires reliability of the production process. Boundaries for the process parameters and constraints for the geometry of the tools require investigation to determine dependable configurations. This paper aimed to investigate the relationships between process parameters, tool geometry, and the occurrence of rupture in the deep-drawing process of paperboard. Different types of ruptures in various phases of the process were distinguished and linked to their specific cause. An extensive experimental investigation with multiple variables of influence was conducted. A logistic regression model was used to describe the experimental data and was statistically validated. The blankholder force was found to be the most influential parameter. Interactions between the parameters blankholder force, punch velocity, and punch diameter were recognized. A high punch velocity can reduce the probability of rupture when the punch diameter is adjusted.

Keywords: Deep-drawing; Paperboard; Logistic regression; Rupture

Contact information: Faculty of Mechanical Science and Engineering, Institute of Processing Machines and Mobile Machines, TU Dresden, Bergstraße 120, 01069 Dresden, Germany;
** Corresponding author: malte.wallmeier@tu-dresden.de*

INTRODUCTION

Approximately 17 million tons of packaging waste was incurred in Germany in 2013. Meanwhile, 88.2% of the 7.8 million tons of paper and paperboard waste and only 49.4% of the 2.9 million tons of plastic waste (Schüler 2015) was recycled. Because packaging waste and recycling are likely to be challenging areas for the next decade, the importance of improving the applicability of paper and paperboard to replace synthetic polymers is imminent. The deep-drawing process of paperboard has been applied for almost a century, since its first detailed investigation by Scherer (1932). On the other hand, the superior formability of synthetic polymers has led to their widespread application above paperboard. However, recent scientific progress has widened the capabilities of paperboard in forming processes and makes paperboard or laminates with a paperboard layer a serious alternative to packaging materials based on synthetic polymers.

Prior to the industrial production of novel deep-drawn packaging products, boundaries for process and material parameters have to be investigated to minimize waste and to ensure the reliability of the production process. For deep drawing of sheet metal, analysis of boundaries for parameters to prevent the production of rejected parts due to quality issues like wrinkles, ruptures and spring back have been conducted already decades ago (Siebel 1954). The primary tool for predicting material failure in deep-drawing is the forming limit diagram, in accordance with the ISO 12004-2 (2008) testing standard. The first attempts to determine the forming limit curves for metal experimentally and theoretically were conducted by Keeler and Backhofen (1964) and Marciniak and Kuczynski (1967). Meanwhile, finite element simulations were widely used in the prediction of the occurrence of rupture during deep-drawing, using models that accounted for the effects of voids in the material (Saxena and Dixit 2011), temperature (Chen *et al.* 2003), or ductile fracture (Lou *et al.* 2012). Unfortunately, fundamental research has not been conducted in the forming of paperboard to a comparable extent.

A closely related forming process of paperboard is hydroforming. In this process, a fluid is required to press a paperboard blank into a forming cavity. The paperboard and fluid are separated with a rubber membrane. Defects, such as cracks, shape inaccuracy, and wrinkles, have been studied (Östlund *et al*. 2011). Relationships between the moisture content, tool temperature, and occurrence of cracks have been elucidated. Undamaged samples were only produced in a narrow range of moisture content because of the increase in strain at brake and the reduction of material stiffness when the moisture content increased. These boundaries of formability in hydroforming are mostly dependent on the extensibility of the paperboard (Vishtal and Retulainen 2014). In Groche and Huttel (2016), methods from sheet metal forming were applied to paperboard hydroforming, *e.g.*, the orientation-based forming limit was determined with an adapted bulge test.

For the deep-drawing of paperboard, empirical models have been developed to investigate and predict the punch force curve (Heinz 1967; Hauptmann 2010). Quality issues have been defined and assigned to different processing parameters (Heinz 1966; Vishtal and Retulainen 2012).

A reduction in the quality can occur because of discoloration, spring-back, deflection of the flange, erratic wrinkling, blister formation, local blackening, or rupture (Hauptmann 2010). Wallmeier *et al*. (2015a) presented a method for an automated detection of wrinkles and investigated the most important process parameters influencing the formation of wrinkles. It was found that the blankholder force was the most important parameter controlling the formation and distribution of wrinkles. Meanwhile, shape accuracy was primarily influenced by the temperature of the tools (Wallmeier *et al.* 2016). Systematic experimental investigations on the occurrence of rupture have yet to be determined.

The aim of this paper was to analyze the occurrence of rupture during the deep-drawing process of paperboard. Ruptures were classified and assigned to a specific causation. An extensive parameter analysis, covering the most important process parameters and geometrical properties of the deep-drawing tools, was investigated, and the logistic regression model was used to describe the experimental data.

EXPERIMENTAL

Methods

All deep-drawing experiments were performed using the equipment at Technische Universität Dresden, Germany, which was described in detail by Hauptmann and Majschak (2011) and Hauptmann (2010). The deep-drawing tools are denoted as the punch, die, and blankholder throughout this publication; the die representing the female part, and the punch representing the male part.

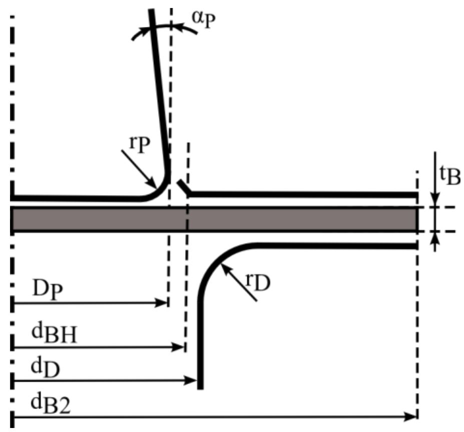

Fig. 1. Schematic representation of the deep drawing tools (Wallmeier *et al.* 2015b)

A schematic representation of the deep drawing tools is given in
Fig. **1**. The values of $\alpha_P = 0.5°$, $r_D = 3\ mm$, $d_D = 110\ mm$ and $d_{B2} = 160\ mm$ were kept constant for all experiments. The abbreviations used in this publication are listed in Table 1.

Table 1. Deep-Drawing Tools

Term	Abbreviation
Diameter of the punch	D_P
Radius at the edge of the punch	r_P
Conicity of the punch	α_P
Radius of the die	r_D
Paperboard thickness	t_B
Diameter of the die	d_D
Diameter of the blank	d_{B2}
Inner diameter of the blankholder	d_{BH}
Punch velocity	v_P
Punch temperature	T_P
Die temperature	TD
Blankholder force	F_{Bh}
Radius at the edge of the punch	r_P
Standard error	SE
Polytetrafluoroethylene (Teflon™)	PTFE

Several parameters were investigated using a range of values to study the occurrence of rupture in the deep-drawing process of paperboard. The most prominent process parameters are the blankholder force, the punch temperature, and the die temperature. A range of punch velocity was also evaluated. The punch radius, die surface, and punch diameter were parameters of the processing tools. All material parameters were kept constant, except for the moisture content. All experiments were performed at 23 ± 1.5 °C and a relative humidity of 50 ± 3%. Six percent moisture content resulted from storing in a temperature of 23 °C and a relative humidity (RH) of 50%, and 11.3% moisture content resulted from storing at 40 °C and 85% RH. The moisture content of the samples was measured according to the ISO 287 (2009) testing standard. All of the experiments were performed on materials from a single batch. The material was a three-layered, fresh fiber paperboard of 350 g m^{-2} (Trayforma Natura) from Stora Enso, Imatra, Finland. A linear reduction in the blankholder force during the infeed of the material in the gap between the punch and the die was utilized throughout the experiment. The blankholder force was the initial force applied when the punch touched the material. As the punch draws the material into the die, the blankholder force was reduced linearly to 500 N until the blank was drawn out of the blankholder.

Table 2. Parameters, Types, and Levels for the Experiments

<table>
<tr><td>Parameter</td><td>Type</td><td colspan="12">Levels/Limits</td></tr>
<tr><td>T_P, °C</td><td rowspan="5">Continuous numeric</td><td colspan="6">80</td><td colspan="6">200</td></tr>
<tr><td>T_D, °C</td><td colspan="6">80</td><td colspan="6">200</td></tr>
<tr><td>Initial F_{BH}, N</td><td colspan="6">500</td><td colspan="6">10000</td></tr>
<tr><td>Moisture content, %</td><td colspan="6">6</td><td colspan="6">11.3</td></tr>
<tr><td>V_P, mm s^{-1}</td><td colspan="6">5</td><td colspan="6">300</td></tr>
<tr><td>r_P, mm</td><td rowspan="2">Discrete numeric</td><td colspan="4">0.2</td><td colspan="4">0.5</td><td colspan="4">5</td></tr>
<tr><td>D_P, mm</td><td colspan="3">108.5</td><td colspan="3">109.1</td><td colspan="3">109.2</td><td colspan="3">109.3</td></tr>
<tr><td>Die surface</td><td>categorical</td><td colspan="6">Polished steel</td><td colspan="6">PTFE-coated</td></tr>
</table>

PTFE: Polytetrafluoroethylene (Teflon™)

The parameters tool temperature, blankholder force, moisture content, and punch velocity can be arbitrarily controlled by the operator. Table 2 lists only the boundaries for the variation of the continuous numeric parameters. Several additional levels were included in the experiments. For example, experiments were conducted with a punch velocity of 5, 10, 20, 50, and 300 mm s^{-1}. All of the levels for the discrete numeric and categorical parameters are listed in Table 2. Numerical values have to be associated with the levels of the categorical parameter for the calculation of the probability of rupture. The steel-coated die was denoted by 1.0, and the PTFE-coated die was denoted by -1.0.

Modes of Rupture

Rupture in the deep-drawing of paperboard is not attributed to a singular reason, *i.e.*, several sources for defects can be found. Table 3 lists the most important modes of rupture and the associated explanation.

Table 3. Rupture in the Deep-Drawing Process and their Explanation

Rupture mode	Rupture	Explanation
A	Rupture occurs at the radius of the punch	The initial blankholder force was too high. The drawing clearance was too small.
B	Rupture at the edge of the cup	A reduction of blankholder force not sufficient. The local pressure at the edge of the flange was too high.
C	Rupture during the in-feed process	The friction coefficient between the punch and the paperboard was lower than the friction coefficient between the die and the paperboard.
D	Material destruction at the edge of the flange	The conical angle of the punch was too small. Compression of the paperboard in the drawing gap exceeded the material's strength.

Examples of the different modes of rupture are shown in Fig. 2. Ruptures in Figs. 2a, b and d were provoked with a toolset with a diameter of the die of 110 mm, whereas Fig. 2c originates from a toolset with a diameter of the die of 80 mm. Rupture mode A demonstrates that the material has not been drawn into the die (Fig. 2a). The excessive blankholder force lead to a rupture at the edge of the punch. Rupture mode B was initiated with the blankholder force kept constant for the whole process at F_{BH} = 13500 N (Fig. 2b). The local compression at the edge of the cup exceeded the materials tensile strength. An evaluation of the pressure under the blankholder at a constant blankholder force and a reduced blankholder force was shown by Wallmeier *et al.* (2015b). Rupture mode C was similar to that of rupture mode A (Fig. 2c). Preliminary experiments demonstrated that the coating of the die's surface can lower the risks of rupture when the friction coefficient between the paperboard and the die decreases. Lowering the coefficient between the punch and the paperboard appeared to be disadvantageous. When the gap between the punch and the die was too narrow, a similar form of rupture during the infeed process originated. Rupture mode D utilized a punch with D_P = 109.3 mm, a conical angle of 0.3°, and F_{BH} = 500 N (Fig. 2d). This form of failure suffered the greatest damage.

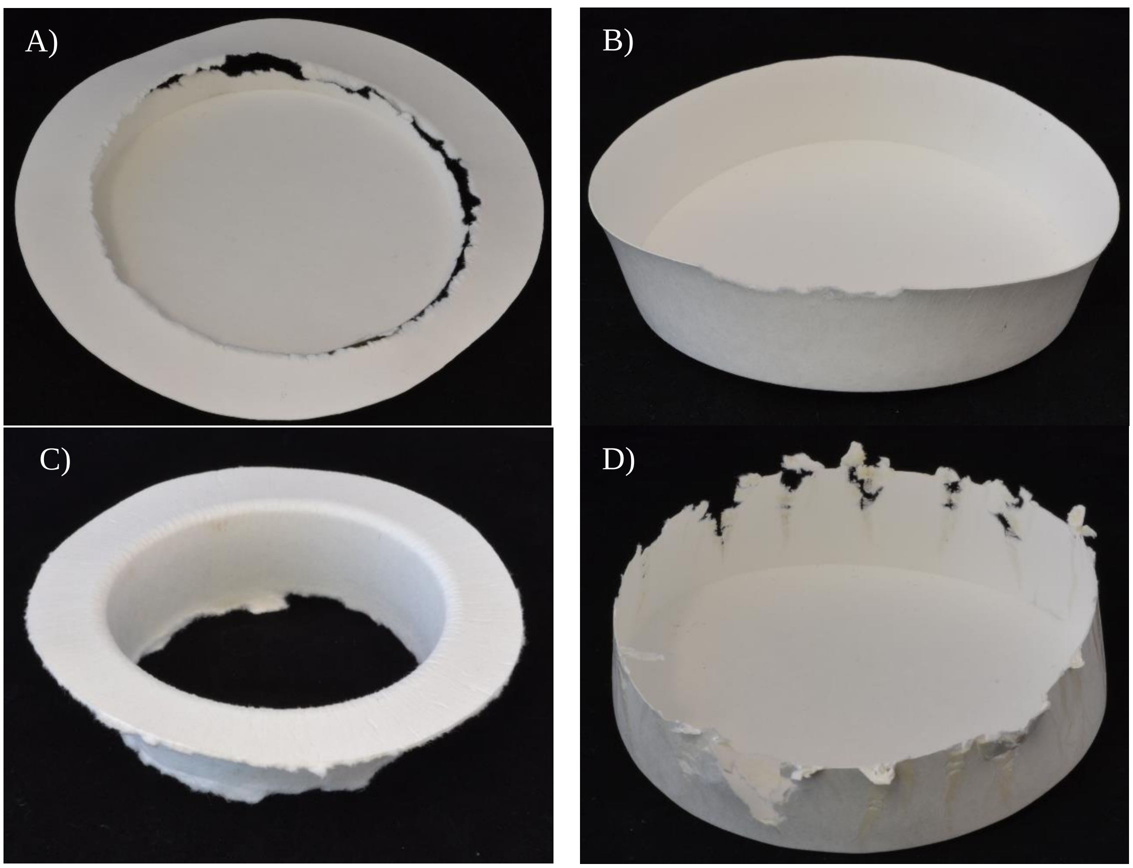

Fig. 2. Examples for a) rupture mode A, b) rupture model B, c) rupture model C, and d) rupture model D

Statistical Method

Material failure is not a continuously defined output variable. The rupture was examined according to two conditions: the deep-drawn cup was intact or the deep-drawn cup was damaged. This binary outcome was used to predict the linear model by logistic regression (Backhaus *et al.* 2011). The theory and application of the logistic regression was described by Hosmer *et al.* (2013). When multiple categories occur, *e.g.*, in different modes of rupture, a multinomial logistic regression can be employed. The logistic regression estimates the relationship between the probability for occurrence of a categorical output variable and one or more independent variables. Consequently, a function z defines the condition of the output variable y, as follows:

$$y = \begin{cases} 1 \; if \; z > 0 \\ 0, \; otherwise \end{cases} \tag{1}$$

The core of the logistic regression is to find the parameter b_j for the independent variable x_j of a function z, where u is the error distributed by the standard logistic distribution (Eq. 2).

$$z = b_0 + \sum_{j=1}^{J} b_j x_j + u \tag{2}$$

The logistic function $\pi(z)$ in Eq. 3 can be utilized to link the function z in Eq. 2 and the output variable.

$$\pi(z) = \frac{e^z}{1 + e^z} = \frac{1}{1 + e^{-z}} \tag{3}$$

Figure 3 shows the logistic function π over the variable x for different values of b_0 and b_1. The function returns values between 0 and 1, and forms a transition zone between them, depending on parameter b_1.

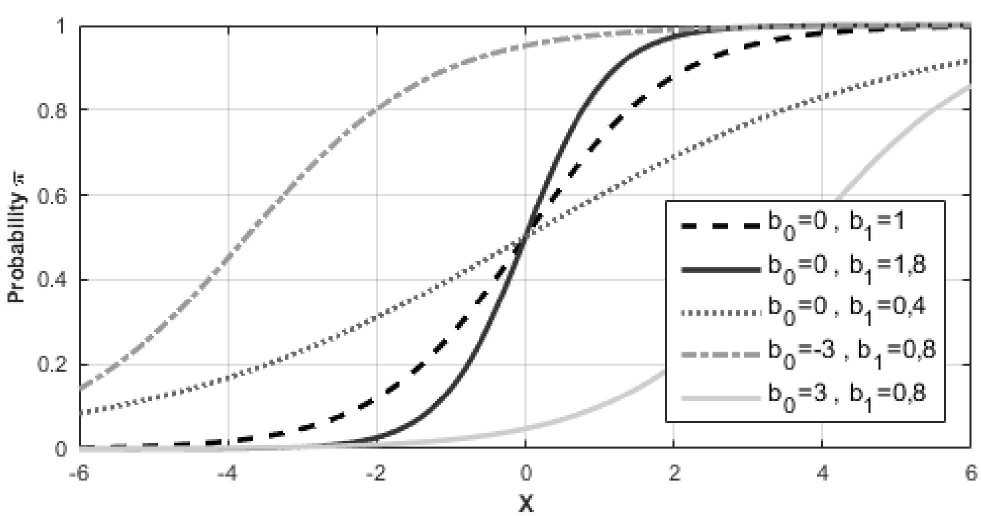

Fig. 3. Logistic function with different parameters, b_0 and b_1

The following equations were limited to one independent variable, to minimize the complexity. The odds of the occurrence of a condition can be interpreted by the fitted values. The odds of a specific state are defined as the ratio of the probability to its complement (Eq. 4).

$$Odds = \frac{\pi(z)}{1-\pi(z)} = e^{b_0+b_1x} \tag{4}$$

The odds ratio is defined as the ratio of the odds of two adjacent levels of a parameter, *e.g.*, the odds of rupture at F_{BH} = 5001 N divided by the odds of rupture at F_{BH} = 5000 N (Eq. 5).

$$Odds\ ratio = \frac{Odds(x+1)}{Odds(x)} = e^{b_1} \tag{5}$$

Consequently, the odds ratio increases in probability for conditions 1 or 0 by one unit change (*e.g.*, the increase in probability of rupture when the blankholder force increased by 1 N). Therefore, the odds ratio depended on the range and the chosen unit, making it difficult to interpret. The odds ratio of a unit change c (*e.g.* 1000 N) can be determined using Eq. 6:

$$Odds\ ratio(c) = e^{cb_1} \tag{6}$$

It follows that increasing the parameter of influence with the hypothetical regression estimate of $b_1 = 0.05$ by 10 leads to a 1.65 times higher probability for the occurrence of condition 0 or 1 (*e.g.*, $Odds\ ratio(10) = e^{10*0.05} = 1.65$).

The Wald-test was utilized for the statistical analysis of the predictor variables. The Wald statistic is similar to a t-test of linear models because it is defined as the squared estimate divided by the squared standard error (Hosmer *et al*. 2013) (Eq. 7).

$$\chi^2{}_j = \frac{{b_j}^2}{{SE_{b_j}}^2} \tag{7}$$

Consequently, a high X^2 value is a good indication that the null hypothesis can be rejected. The P-value is the probability of obtaining the calculated χ^2-value or a higher one assuming that the corresponding parameter has no influence on the outcome of the experiments. Significance was accepted at the $P < 0.05$ significance level.

The statistical analysis and the reporting of the results was executed following the recommendations from Peng *et al.* (2002). The evaluation of the logistic regression model was conducted in three steps. First, a whole model test and a lack-of-fit test were conducted to check the validity of the overall model. Then, the individual predictors were tested with a Wald-test, utilizing the X^2 statistic. Finally, the predicted probabilities were validated using a random range of testing points. A table with the predicted probabilities and the observed ruptures is presented in Appendix A. The statistical analysis was conducted using SAS Institute Inc. JMP® Pro 11.1.1 (64-bit, Cary, NC).

RESULTS AND DISCUSSION

Validation of the Model

Experiments were performed with the parameters and levels from Table 2, resulting in 417 testing points. All experimental points were repeated, at minimum, three times. There were 246 ruptures that occurred in the tests, and 171 samples were undamaged. The results of the logistic regression model are presented in Table 4. The odds ratios for the categorical variable die surface are listed in Table 5.

Table 4. Parameter Estimates, X^2 values, P-values, and Odds Ratios for the Logistic Regression Model

Term	Estimate b_j	SE	χ^2	P-value	Odds ratio
Intercept b_0	1246.8	313.14	15.85	< 0.0001	Not defined
Punch temperature	0.0148	0.00404	13.59	0.0002	1.015
Die temperature	-0.00137	0.00412	0.11	0.740	NS
Blankholder force	0.00104	0.000136	58.27	< 0.0001	1.00104*
Punch radius	0.0967	0.1001	0.93	0.334	NS
Die surface	-1.015	0.219	21.44	< 0.0001	Table 5
Moisture content	-0.145	0.0929	2.44	0.118	NS
Punch velocity	-0.00582	0.00243	5.75	0.0165	0.9942*
Punch diameter	-11.48	2.873	15.98	< 0.0001	1.031^{-5}*
Blankholder force x Punch diameter	-0.00404	0.00107	14.33	0.0002	Not defined
Punch velocity x Punch diameter	0.0590	0.0172	11.78	0.0006	Not defined

*derived from model without interaction terms. NS: not significant

A full model test was conducted, and the model was found to be statistically significant. This indicated that the inclusion of the parameters improved the prediction of the model in comparison to an intercept-only model ($X^2(10) = 246.9$, $P < 0.0001$). A lack-of-fit test was used to evaluate whether the chosen model contained enough information with the current variables. "It calculates a pure-error negative log-likelihood by constructing categories for every combination of the regressor values in the data and it tests whether this log-likelihood is significantly better than the fitted model," (SAS Institute Inc. 2014). The insignificant lack-of-fit X^2-value shows that the additional terms, *e.g.*, the polynomial or the interaction terms, were not significant ($X^2(113) = 134.5$, $P = 0.0783$); therefore, these terms do not improve the prediction of the model. A model without the interaction terms resulted in $X^2(115) = 160.1$, $P = 0.0035$, and this model indicated that the interaction terms have to be included because of the low P-value. Most of the randomly chosen experiments from Appendix A were predicted correctly. Of course, the prediction of probability for parameter combinations that lay in the transition zone between reliable production and high probability of rupture is exceptionally difficult. Therefore, parameter settings for industrial production should be chosen with a probability of rupture that does not exceed approximately 10%. It should also be noted that experiments were conducted covering a wide range for each parameter. In future examinations, the number and the range of parameters could be reduced to improve the prediction of the model within the critical zone.

Parameters of Influence

The parameters moisture content and die temperature were found to be statistically insignificant, which was indicated by the results of a Wald-test ($X^2(1) = 0.11$, $P = 0.74$; $X^2(1) = 2.44$, $P = 0.118$). Furthermore, the punch radius did not exhibit a significant influence on the rupture ($X^2(1) = 0.93$, $P = 0.334$) of the material. For brittle materials, the punch radius could have been influenced by damage occurring at sharp edges, which reduces the endurable tensile load (Hauptmann *et al.* 2015). There are different possible reasons for the insignificance of a parameter. Firstly, the parameter could be truly statistically insignificant. This would be especially surprising for the moisture content, which is influential on the tensile properties of paper (Yeh *et al.* 1991). The insignificance of the die temperature would also be surprising because of the findings by Linvill and Östlund (2014), concerning the combined effects of temperature and moisture on the mechanical properties of paper. Secondly, the variation of these parameters could be insufficient. The die temperature varied between 80 °C and 200 °C, which should lead to effectual changes in the mechanical properties. The moisture content varied between 6.0% and 11.3%, which represents a range that should have influenced the mechanical properties of the paperboard (Yeh *et al.* 1991). Finally, the variation between the results of a singular testing point could exceed the variation between different testing points, resulting in a statistically insignificant effect due to a high standard error. This reason could apply to the die temperature, as well as the moisture content. Samples have to be transferred from the climate cabinet to the testing equipment manually, thus the moisture content is likely to change in the period prior to the experiment. Additionally, the manual infeed process in the machine contains sources of error because the paperboard rests on the heated die for several seconds before the operator starts the process. This may also lead to variations which are likely to mask a significant influence of these parameters.

Table 5. Odds Ratio for the Categorical Variable Die Surface

Level 1	Level 2	Odds ratio
PTFE-coated	Polished steel	7.63
Polished steel	PTFE-coated	0.14

PTFE: Polytetrafluoroethylene (Teflon™)

The Wald-test showed that the blankholder force ($X^2(1) = 58.27$, $P < 0.0001$), punch temperature ($X^2(1) = 13.59$, $P = 0.0002$), and punch diameter ($X^2(1) = 15.98$, $P < 0.0001$) were statistically significant. Changing the surface of the die also exhibited a significant influence on the occurrence of rupture ($X^2(1) = 21.44$, $P < 0.0001$).

The odds ratio can aid in the interpretation of the results. The analysis of odds ratio is not meaningful for parameters that are also included in interaction terms (Hosmer *et al*. 2013). Therefore, the interaction terms were removed from the model, keeping in mind that the lack-of-fit test strongly recommended the inclusion of the interaction terms. All of the other interpretations of the result originated from the model that is presented in Table 4. An increase in the punch temperature of 50 °C made the occurrence of rupture approximately 2 times more likely. Furthermore, increasing the blankholder force 1000 N doubled the odds of rupture. When then punch speed was increased by 100 mm s^{-1}, the odds of rupture declined from 1.0 to 0.83. Changing from PTFE to polished steel reduced the probability of rupture from 1.0 to 0.14.

The *P*-value in Table 4 indicates a strong interaction between the blankholder force and the punch diameter. At $D_P = 108.5$ mm there was a sharp transition from a very low probability of rupture (up to $F_{BH} = 3000$ N) to a high probability of rupture (above approximately $F_{BH} = 5000$ N) (Fig. 4). The sharp transition disappeared when the punch diameter increased. The material thickness was 0.46 mm, the diameter of the die was 110 mm. Consequently, the material was compressed between the punch and the die when the punch diameter exceeded 109.1 mm. In this state, ruptures seemed to occur more randomly. The model predicts ruptures even at a very low blankholder force, but in certain cases, a high blankholder force is applicable. Even at $F_{BH} = 10000$ N, the model predicts a probability of rupture (0.94).

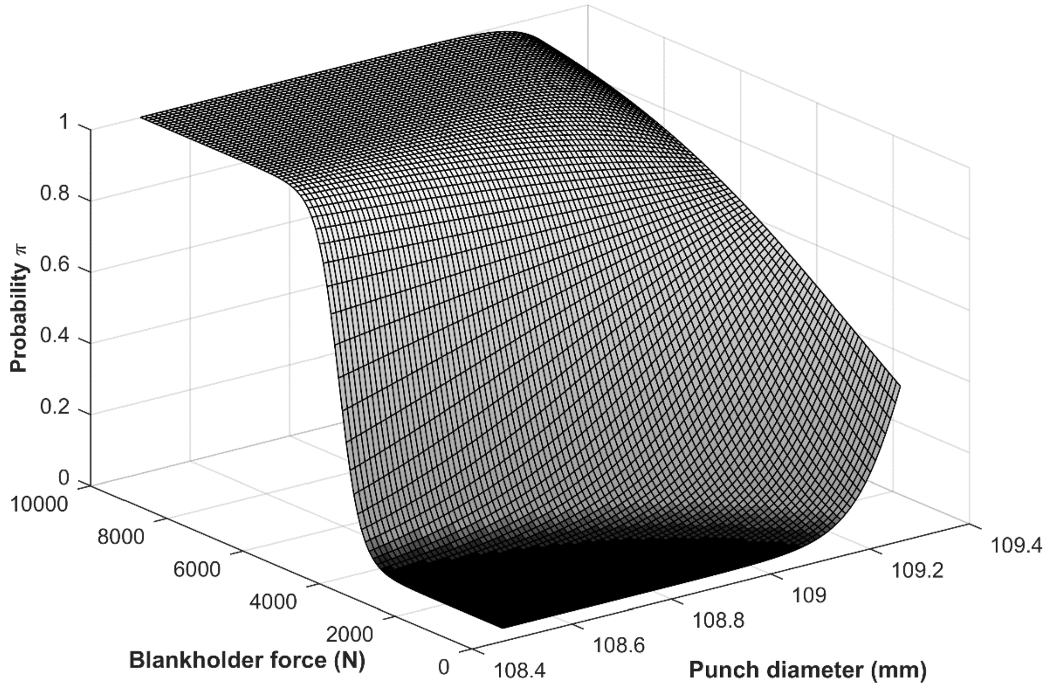

Fig. 4. Probability of rupture demonstrated by the relationship between the blankholder force and the punch diameter, with T_P = 140 °C, PTFE-coated die, and V_P = 180 mm s^{-1}

Figure 5 shows the geometrical conditions when the punch diameter is varied. The tensile load in Fig. 5a) was applied to the same section of paperboard during the entire process.

The material's tensile strength limited the maximal initial blankholder force. In Fig. 5b the material was compressed between the punch and the die. The state of stress changed with additional stress in the through-thickness direction, which seemed to increase the maximum initial blankholder force. Furthermore, shear loading appeared when the material was compressed between the punch and the die.

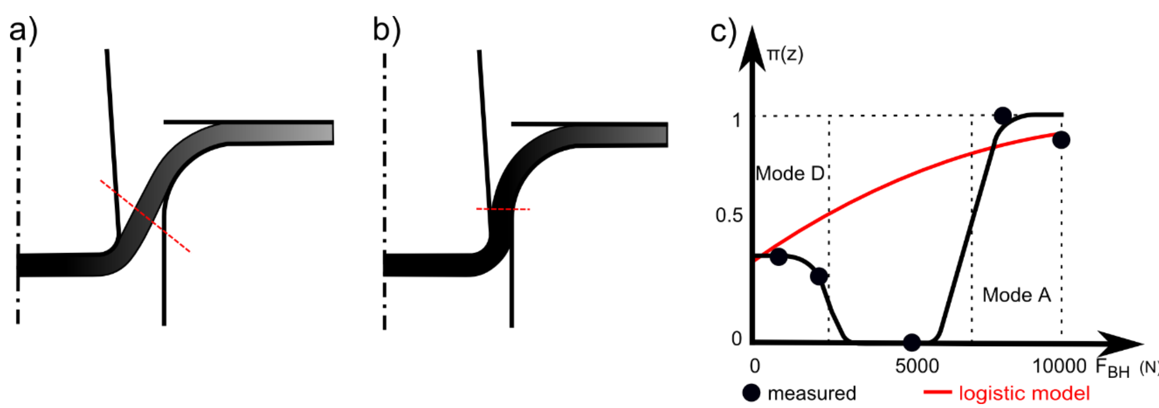

Fig. 5. Schematic of a) the geometry and position of the highest load for D_P = 108.5 mm, b) the geometry and position of the highest load for D_P = 109.3 mm, and c) the behavior at D_P = 109.3 mm

The number of wrinkles was reduced when a low initial blankholder force was applied (Wallmeier *et al.* 2015a). Therefore, more material was compressed into one wrinkle, which locally increased the thickness of the material. When the gap between the punch and the die was minimal, local compression resulted in material destruction and rupture, similar to that of the rupture mode D. Therefore, two different types of ruptures occurred at D_P = 109.3 mm, depending on the drawing gap between the punch and the die. Figure 5C illustrates the behavior that can be assumed but was not predicted by the model. At D_P = 109.3 mm, the logistic regression model could have profited from an additional quadratic term for the blankholder force; however, since the model covers a very wide range of parameters, the quadratic term for the blankholder force was statistically insignificant when all experiments were considered.

Figure 6 shows the probability of rupture for the punch velocity and punch diameter. The model in Table 4 predicts an interaction between these two parameters. The blankholder force of 5000 N was in the transition zone from low to high probability of rupture (Fig. 4). Consequently, there was no zone of low probability of rupture in Fig. 6. It is indicated that a high punch velocity enabled the production of intact cups, while a low punch velocity led to a high probability of rupture (Fig. 6) for $D_P = 108.5$ mm. This can be explained by the effect of strain rate on the in-plane tensile stress-strain behavior of paperboard, whereby increasing the strain rate results in a higher tensile strength and a higher *e*-modulus (Andersson and Sjöberg 1953; Gustafsson and Niskanen 2012).

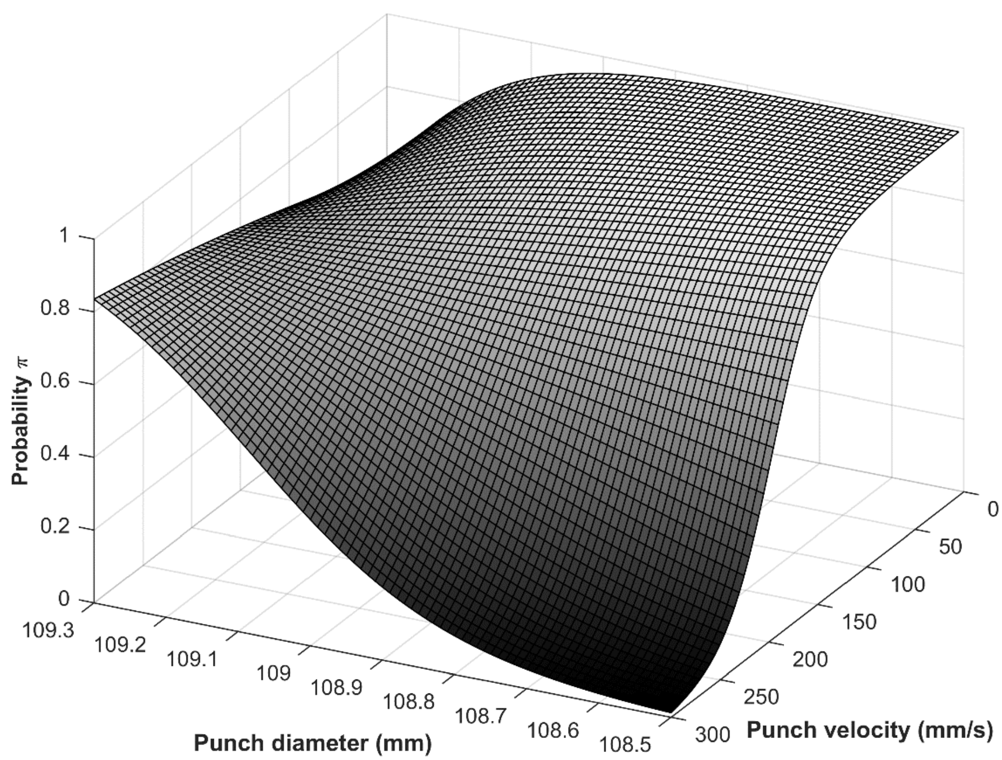

Fig. 6. Probability of rupture demonstrated by the relationship between the punch velocity and the punch diameter, with T_P = 140 °C, PTFE-coated die, and F_{Bh} = 5000 N

The significance of the interaction term for punch velocity and punch diameter indicated that a positive effect of high punch velocity did not exist upon compression. In this case, a lower punch velocity may prevent rupture mode C. The p-values for the interaction term and punch velocity (p = 0.0165 and p = 0.0006) were high compared to the p-value of the term of blankholder force. Therefore, the results concerning the punch velocity should be interpreted with special care.

The probability of rupture for the interaction of the blankholder force and the punch temperature is shown in Fig. 7. The effect of punch temperature on the probability of rupture is shown. Additionally, the blankholder force is plotted in Fig. 7 to clarify the influence of punch temperature. High punch temperature leads to a reduction in the applicable blankholder force or increases the probability of rupture at constant blankholder force. This can be explained by the softening effect of temperature on the paperboard (Salmén and Back 1977; Salmén 1982).

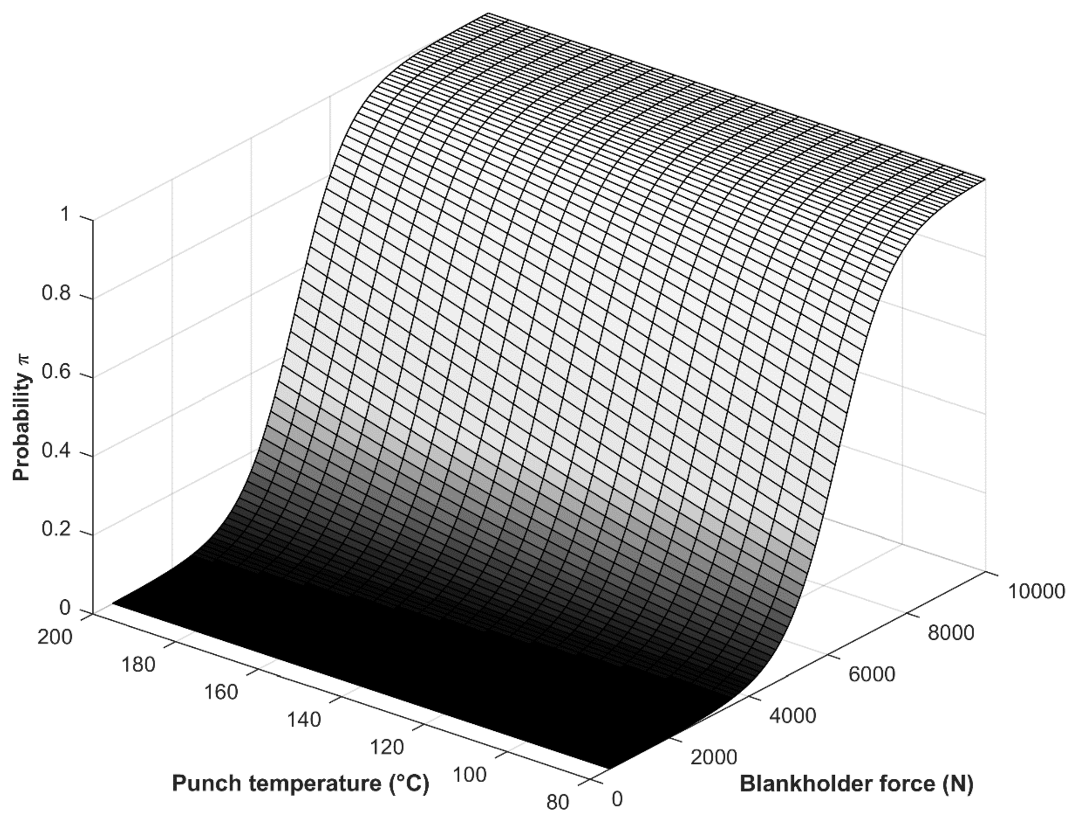

Fig. 7. Probability of rupture demonstrated by the relationship between the blankholder force and the punch temperature, with PTFE-coated die, D_P = 109.0 mm, and V_P = 180 mm s^{-1}

A statistically significant effect of the die temperature was not found, even though the material was in contact with the die for a longer period of time compared with that of the punch. This behavior can easily be explained when the paperboard is not compressed between the punch and the die because the die has, in this case, no contact with the zone of rupture at the edge of the punch. The rupture mode C is likely to be influenced by the die temperature, but the chosen tools generally prohibited the occurrence of this rupture mode. Changes in tool temperature exhibit an additional effect on the geometrical conditions through thermal expansion. While increased punch temperature reduces the gap between the punch and the die, increasing the die temperature enlarges this gap. The punch diameter exhibits a strong influence on the probability of rupture; thus, a reduced gap between the punch and the die increases the odds of rupture in many cases. To examine this hypothesis, the gap between the punch and the die was calculated for all experiments considering the thermal expansion of the tools; however, a statistically significant relationship was not found for the temperature-induced changes in the drawing gap.

The last parameter of influence was the surface of the die. Figure 8 shows the effect of the surface of the die on the probability of rupture for different blankholder forces.

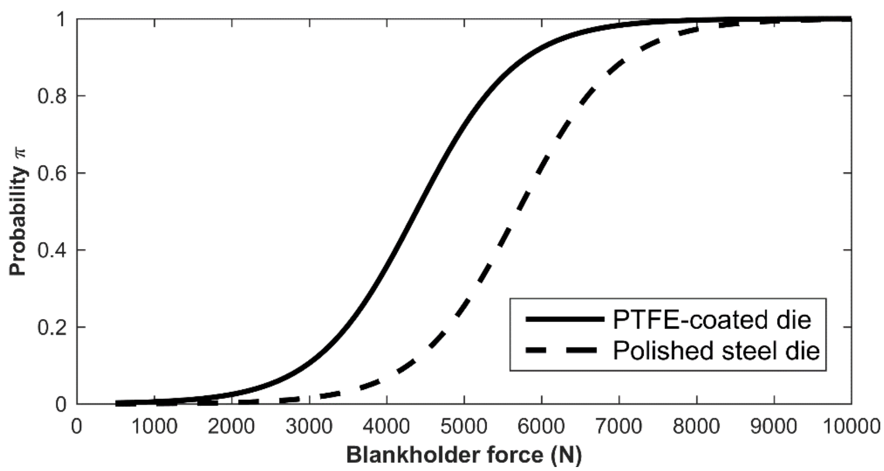

Fig. 8. Probability of rupture by the blankholder force for PTFE-coated *versus* polished steel die, with T_P = 140°C, D_P = 109.0 mm, and V_P = 180 mm s^{-1}

Originally, all of the tools were made from polished steel. Figure 8 shows that the PTFE-coating produced inferior results concerning the probability of rupture. Furthermore, the friction between the die and the paperboard led to deterioration of the PTFE-coating.

The logistic regression was found to be a suitable representation of the model for the occurrence of rupture in the deep-drawing process of paperboard. Relationships between the most influential parameters were discovered. In this first investigation, a large number of parameters covering a wide range of options were tested. Therefore, the model had to predict ruptures that arose from different causes with only 11 parameters. Even though the statistical tests provided a good fit of the model, they did not capture all of the effects. Consequently, the quality of the prediction was insufficient in some portions of the parameter range. Thus, further investigations regarding rupture should be executed, concentrating on the transition zones between reliable production and high probability of rupture. The changes emerging from the compression of the paperboard between the punch and the die require further study.

After including these additional results, the empirical model may be able to predict the probability of rupture for the most important process parameter and tool design features. It can then be used for optimization of the tool design and troubleshooting process parameters. Additionally, the model provides further information for the understanding of the impact of process parameters and tool design features on the forming process.

CONCLUSIONS

1. Logistic regression can be utilized to generate an empirical model that predicts the probability for the occurrence of rupture during the deep-drawing process of paperboard.
2. A whole model test and a lack-of-fit test were used to validate the model. The model was well-described and predicted the occurrence better than an intercept-only model.
3. Different modes of rupture during the deep-drawing process can be distinguished and assigned to a specific cause.
4. The blankholder force was the most influential parameter concerning the occurrence of rupture.
5. Statistically significant ($P < 0.05$) interactions between the blankholder force, punch velocity, and punch diameter were found.
6. A high punch velocity was beneficial for the reduction of the probability rupture when the material does not experience z-directional compression by the tools.
7. The conditioning of the surface of the die influences the occurrence of rupture. The polished steel surface was superior to the PTFE-coated surface.
8. No significant influence ($P > 0.05$) was found for the die temperature, punch radius, and moisture content on the rupture property of paperboard.

ACKNOWLEDGMENTS

The authors are grateful for the generous support from StoraEnso.

REFERENCES CITED

Andersson, O., and Sjöberg, L. (1953). "Tensile studies of paper at different rates of elongation," *Svensk Papperstidning* 56(16), 615-624.

Backhaus, K., Erichson, B., Plinke, W., and Weiber, R. (2011). *Multivariante Analysemethoden*, Springer-Lehrburg, Berlin. DOI: 10.1007/978-3-642-16491-0

Chen, F.-K., Huang, T.-B., and Chang, C.-K. (2003). "Deep drawing of square cups with magnesium alloy AZ31 sheets," *International Journal of Machine Tools & Manufacturing* 43(15), 1553-1559. DOI: 10.1016/S0890-6955(03)00198-6

Groche, P., and Huttel, D. (2016). "Paperboard forming - Specifics compared to sheet metal forming," *BioResources* 11(1), 1855-1867. DOI: 10.15376/biores.11.1.1855-1867

Gustafsson, P.-J., and Niskanen, K. (2012). "Paper as an engineering material," in: *Mechanics of Paper Products*, K. Niskanen (ed.), De Gruyter, Berlin, pp. 5-26. DOI: 10.1515/9783110254631.5

Hauptmann, M. (2010). *Die Gezielte Prozessführung und Möglichkeiten zur Prozessüberwachung beim Mehrdimensionalen Umformen von Karton durch Ziehen*, Ph.D. Thesis, Technische Universität Dresden, Dresden, Germany.

Hauptmann, M., and Majschak, J.-P. (2011). “New quality level of packaging components from paperboard through technology improvement in 3D forming,” *Packaging Technology & Science* 24(7), 419-432. DOI: 10.1002/pts.941

Hauptmann, M., Wallmeier, M., Erhard, K., Zelm, R., and Majschak, J.-P. (2015). “The role of material composition, fiber properties and deformation mechanism in deep drawing of paperboard,” *Cellulose* 22(5), 3377-3395. DOI: 10.1007/s10570-015-0732-x

Heinz, O. (1966). “Ungenügende Ziehqualität und ihre Ursachen [Insufficient quality of deep-drawn samples and associated causes],“ *Papier und Druck, Fachteil Buchbinderei* 6, 89-95.

Heinz, O. (1967). “Ziehkraftdiagramme beim Ziehen von Karton und Pappe, [Force-time diagram for deep.drawing of paperboard],“ *Papier und Druck, Fachteil Buchbinderei und Papierverarbeitung* 8, 136-139.

Hosmer, D. W., Lemeshow, S., and Sturdivant, R. X. (2013). *Applied Logistic Regression* 3rd ed., John Wiley & Sons Inc., Hoboken, NJ. DOI: 10.1002/0471722146

ISO 287:2009 (2009). “Paper and board - Determination of moisture content of a lot - Oven-drying method,” ISO, Geneva, Switzerland

ISO 12004-2:2008 (2008). “Metallic materials - Sheet and strip - Determination of forming-limit curves - Part 2: Determination of forming-limit curves in the laboratory,” ISO, Geneva, Switzerland

Keeler, S. P., and Backhofen, W. A. (1964). “Plastic instability and fracture in sheet stretched over rigid punches,” *ASM Transactions Quarterly* 56(1), 25-48.

Linvill, E., and Östlund, S. (2014). “The combined effects of moisture and temperature on the mechanical response of paper,” *Experimental Mechanics* 54(8), 1329-1341. DOI: 10.1007/s11340-014-9898-7

Lou, Y., Huh, H., Lim, S., and Pack, K. (2012). “New ductile fracture criterion for prediction of fracture forming limit diagrams of sheet metals,” *International Journal of Solids & Structures* 49(25), 3605-3615. DOI: 10.1016/j.ijsolstr.2012.02.016

Marciniak, Z., and Kuczynski, K. (1967). “Limit strains in the processes of stretch-forming sheet metal,” *International Journal of Mechanical Sciences* 9(9), 609-620. DOI: 10.1016/0020-7403(67)90066-5

Östlund, M., Borodulina, S., and Östlund, S. (2011). “Influence of paperboard structure and processing conditions on forming of complex paperboard structures,” *Packaging Technology & Science* 24(6), 331-341. DOI: 10.1002/pts.942

Peng, C.-Y. J., Lee, K. L., and Ingersoll, G. M. (2002). “An introduction to logistic regression analysis and reporting,” *Journal of Educational Research* 96(1), 3-14. DOI: 10.1080/00220670209598786

Salmén, L. (1982). *Temperature and Water Induced Softening Behaviour of Wood Fiber Based Materials*, Ph.D. Thesis, The Royal Institute of Technology, Stockholm, Sweden.

Salmén, L., and Back, E. (1977). “Simple stress-strain measurements on dry papers from -25 °C to 250 °C,” *Svensk Papperstidning* 80(6), 178-183.

SAS Institute Inc. (2014). *JMP 11 Fitting Linear Models*, SAS Institute Inc., Cary, NC.

Saxena, R. K., and Dixit, P. M. (2011). “Numerical analysis of damage for prediction of fracture initiation in deep drawing,” *Fine Elements in Analysis & Design* 47(9), 1104-1117. DOI: 10.1016/j.finel.2011.04.003

Scherer, K. (1932). *Untersuchungen über Ziehfähigkeit und den Ziehvorgang von Pappe* [*Investigation of formability and forming of paperboard*], Ph.D. Thesis, Technische Hochschule zu Dresden, Dresden, Germany.

Schüler, K. (2015). *Aufkommen und Verwertung von Verpackungsabfällen in Deutschland im Jahr 2013*, Umweltbundesamt (Ed.) Dessau-Roßlau, Umweltbundesamt.

Siebel, E. (1954). "Der Niederhalterdruck beim Tiefziehen [Blankholder force during deep drawing]," *Stahl und Eisen* 74(3), 155-158.

Vishtal, A., and Retulainen, E. (2012). "Deep-drawing of paper and paperboard: The role of material properties," *BioResources* 7(3), 4424-4450. DOI: 10.15376/biores.7.3.4424-4450

Vishtal, A., and Retulainen, E. (2014). "Boosting the extensibility potential of fibre networks - A review," *BioResources* 9(4), 7933-7983. DOI: 10.15376/biores.9.4.7933-7983

Wallmeier, M., Hauptmann, M., and Majschak, J.-P. (2015a). "New methods for quality analysis of deep-drawn packaging components from paperboard," *Packaging Technology & Science* 28(2), 91-100. DOI: 10.1002/pts.2091

Wallmeier, M., Linvill, E., Hauptmann, M., Majschak, J.-P., and Östlund, S. (2015b). "Explicit FEM analysis of the deep drawing of paperboard," *Mechanics of Materials* 89, 202-215. DOI: 10.1016/j.mechmat.2015.06.014

Wallmeier, M., Noack, K., Hauptmann, M., and Majschak, J.-P. (2016). "Shape accuracy analsis of deep drawn packaging components made of paperboard," *in Press Nordic Pulp and Paper Research Journal*.

Yeh, K. C., Considine, J. M., and Suhling, J. C. (1991). "The influence of moisture content on the nonlinear constitutive behavior of cellulosic materials," in: *Proceedings of the 1991 International Paper Physics Conference*, TAPPI, Kona, Hawaii, pp. 695-711.

Article submitted: February 22, 2016; Peer review completed: March 31, 2016; Revised version received and accepted: April 1, 2016; Published: April 12, 2016.
DOI: 10.15376/biores.11.2.4688-4704

APPENDIX A

Table 6. Predicted Probability of Rupture and the Results

F_{BH} (N)	T_P (°C)	Die surface	v_P (mm s^{-1})	D_P (mm)	Rupture	Prediction
3000	80	Polished steel	20	109.2	0.0	0.042
4000	200	Polished steel	20	109.2	0.0	0.355
6000	200	Polished steel	20	109.2	1.0	0.706
5000	80	PTFE-coated	50	109.2	1.0	0.584
5000	160	PTFE-coated	5	109.2	0.4	0.832
5000	80	Polished steel	5	109.2	0.4	0.164
10000	160	Polished steel	300	109.1	1.0	0.984
500	80	Polished steel	300	109.3	0.0	0.057
7625	80	Polished steel	10	108.5	1.0	1.000
3000	80	PTFE-coated	5	109.2	0.0	0.183
7625	80	Polished steel	300	109.1	1.0	0.547
9000	160	PTFE-coated	5	109.2	1.0	0.990

All experiments with identical parameter combination had the same result
The occurrence of rupture is denoted 1.0
Intact samples are denoted as 0
Intact and defective samples were produced with one parameter combination and the result was the ratio of intact to defective samples
PTFE: Polytetrafluoroethylene (Teflon™)